Supplemental Material can be found at:
http://www.mcponline.org/cgi/content/full/M500089-MCP200/DC1

Time-resolved Mass Spectrometry of Tyrosine Phosphorylation Sites in the Epidermal Growth Factor Receptor Signaling Network Reveals Dynamic Modules*[S]

Yi Zhang‡§, Alejandro Wolf-Yadlin‡§, Phillip L. Ross¶, Darryl J. Pappin¶, John Rush‖, Douglas A. Lauffenburger‡, and Forest M. White‡**

Ligand binding to cell surface receptors initiates a cascade of signaling events regulated by dynamic phosphorylation events on a multitude of pathway proteins. Quantitative features, including intensity, timing, and duration of phosphorylation of particular residues, may play a role in determining cellular response, but experimental data required for analysis of these features have not previously been available. To understand the dynamic operation of signaling cascades, we have developed a method enabling the simultaneous quantification of tyrosine phosphorylation of specific residues on dozens of key proteins in a time-resolved manner, downstream of epidermal growth factor receptor (EGFR) activation. Tryptic peptides from four different EGFR stimulation time points were labeled with four isoforms of the iTRAQ reagent to enable downstream quantification. After mixing of the labeled samples, tyrosine-phosphorylated peptides were immunoprecipitated with an anti-phosphotyrosine antibody and further enriched by IMAC before LC/MS/MS analysis. Database searching and manual confirmation of peptide phosphorylation site assignments led to the identification of 78 tyrosine phosphorylation sites on 58 proteins from a single analysis. Replicate analyses of a separate biological sample provided both validation of this first data set and identification of 26 additional tyrosine phosphorylation sites and 18 additional proteins. iTRAQ fragment ion ratios provided time course phosphorylation profiles for each site. The data set of quantitative temporal phosphorylation profiles was further characterized by self-organizing maps, which resulted in identification of several cohorts of tyrosine residues exhibiting self-similar temporal phosphorylation profiles, operationally defining dynamic modules in the EGFR signaling network consistent with particular cellular processes. The presence of novel proteins and associated tyrosine phosphorylation sites within these modules indicates additional components of this network and potentially localizes the topological action of these proteins. Additional analysis and modeling of the data generated in this study are likely to yield more sophisticated models of receptor tyrosine kinase-initiated signal transduction, trafficking, and regulation. ***Molecular & Cellular Proteomics 4:1240–1250, 2005.***

Cell signaling downstream of receptor tyrosine kinases, such as epidermal growth factor receptor (EGFR),[1] comprises an interconnected network of pathways associated with various regulatory processes. These pathways involve a number of components whose interactions are required to carry out regulatory processes and that are themselves regulated by covalent modifications, including phosphorylation on tyrosine as well as serine and threonine residues. In the particular case of EGFR, ligand binding activates the receptor and dimerization results in autophosphorylation of selected tyrosine sites in the C-terminal region (1). Different tyrosine phosphorylation sites in EGFR (*i.e.* Tyr-1092 and Tyr-1110 for Grb2 (2), Tyr-1172 and Tyr-1197 for SHC (3)) act as docking sites for a variety of proteins upstream of several signaling cascades, most prominently mitogen-activated protein kinase, phospholipase C-γ, and phosphoinositide 3-kinase pathways, leading to proliferation, differentiation, migration, and antiapoptotic effects (4–6). Because EGFR is at the origin of pathways governing diverse cell behavioral responses such as cell survival, proliferation, differentiation, and motility, ascertaining quantitative and dynamic features of the various regulatory pathways will be imperative for determining which features are related to particular responses. Indeed, because dysregulation of EGFR-activated pathways, often a consequence of receptor overexpression or mutation, has been shown to be correlated with many types of cancer, one promising step toward identifying mechanisms underlying tumorigenesis associated with aberrant EGFR signaling would be to generate a quantitative comparison of a broad variety of specific cellular signaling events downstream of this RTK under multiple bio-

From the ‡Biological Engineering Division, Massachusetts Institute of Technnology, Cambridge, Massachusetts 02139, ¶Applied Biosystems, Framingham, Massachusetts 01701, and ‖Cell Signaling Technology, Inc., Beverly, Massachusetts 01915

Received March 28, 2005, and in revised form June 7, 2005
Published, MCP Papers in Press, June 11, 2005, DOI 10.1074/mcp.M500089-MCP200

[1] The abbreviations used are: EGFR, epidermal growth factor receptor; SOM, self-organizing map; IP, immunoprecipitation.

© 2005 by The American Society for Biochemistry and Molecular Biology, Inc.
This paper is available on line at http://www.mcponline.org

Downloaded from www.mcponline.org at Francis A. Countway Library of Medicine on October 16, 2007

Molecular & Cellular Proteomics

logical cell states. These data could then be used to implement models of cellular signaling pathways, from which predictions could be made as to the most beneficial intervention strategies. Toward this end, we describe here a quantitative mass spectrometric method for time-resolved analysis of dynamic tyrosine phosphorylation at specific sites on multiple proteins simultaneously, using the EGFR signaling cascade as a model.

All phosphorylation-mediated cellular signaling cascades are bound by the same principles. A dynamic relationship between component proteins in the pathway generates site- and time-specific phosphorylation/dephosphorylation events that propagate down the cascade until the desired response is elicited. Most proteins have more than one potential phosphorylation site, and phosphorylation/dephosphorylation of different sites in the same protein may lead to different responses; *i.e.* activation events may involve a particular protein, but specific phosphorylation sites regulate the cellular activity (7, 8). So far, most of the literature deals with either time dynamics on the activation of a handful of proteins and phosphorylation sites (9, 10) or global identification of protein phosphorylation sites under static conditions (11–14).

Our current knowledge about the EGFR-related pathways dynamics and the phosphorylation sites of their proteins represent the summary of decades of work by many groups using traditional biochemistry tools to study the activation of only several proteins at a time. Only recently has mass spectrometry been used to identify many tyrosine phosphorylation sites in receptor tyrosine kinase pathways (15–18) and to monitor total phosphotyrosine content in pathway proteins over time (19). However, these studies have not provided information on the dynamic regulation of specific tyrosine phosphorylation sites. We have developed a method to provide this level of information and have applied it to the EGFR model system, generating time course phosphorylation profiles for 78 tyrosine phosphorylation sites on 58 proteins at four time points of EGF stimulation (0, 5, 10 and 30 min) in a single analysis. Stimulation and replicate analyses of a separate set of cell cultures were used to validate the data set while providing identification of an additional 26 phosphorylation sites and 18 proteins with associated temporal phosphorylation profiles.

MATERIALS AND METHODS

Cell Culture, EGF Stimulation—184A1 parental human mammary epithelial cells (20) were a kind gift from Martha Stampfer (Lawrence Berkeley Laboratory, Berkeley, CA) and were maintained in DFCI-1 medium supplemented with 12.5 ng/ml EGF, as in Ref. 21. Cells were washed with PBS and incubated for 12 h in serum-free media (DFCI-1 without EGF, bovine pituitary extract, or fetal bovine serum) in 15-cm plates ($\sim 3 \times 10^7$ cells) after 80% confluence was reached. The synchronized cells were washed with PBS after removal of media. The cells were then stimulated with 25 nM EGF in serum-free media without sodium bicarbonate for 5, 10, or 30 min or left untreated with serum-free media for 5 min as control.

Cell Lysis, Protein Digestion, and Peptide Fractionation—After EGF stimulation, cells were lysed on ice with 3 ml of 8 M urea supplemented with 1 mM Na_3VO_4. A 10-μl aliquot was taken from each sample to perform bicinchoninic acid protein concentration assay (Pierce) according to the manufacturer's protocol. Cell lysates were reduced with 10 mM DTT for 1 h at 56 °C, alkylated with 55 mM iodoacetamide for 45 min at room temperature, and diluted to 12 ml with 100 mM ammonium acetate, pH 8.9. 40 μg of trypsin (Promega) was added to each sample ($\sim$100:1 substrate/trypsin ratio), and the lysates were digested overnight at room temperature. The whole-cell digest solutions were acidified to pH 3 with acetic acid (HOAc) and loaded onto C18 Sep-Pak Plus Cartridges (Waters). The peptides were desalted (10 ml of 0.1% HOAc) and eluted with 10 ml of a solution composed of 25% acetonitrile (MeCN) with 0.1% HOAc. Each sample was divided into 10 aliquots and lyophilized overnight to dryness for storage at −80 °C.

iTRAQ Labeling and Peptide IP—Peptide labeling with iTRAQ reagent (Applied Biosystems) was performed according to the manufacturer's protocol. In brief, each aliquot (3×10^6 cell equivalent) was reacted with one tube of iTRAQ reagent; *i.e.* acquisition of this data set from the first biological sample required 8 tubes of iTRAQ reagent (2 × iTRAQ-114 (0 min), 2 × iTRAQ-115 (5 min), 2 × iTRAQ-116 (10 min), and 2 × iTRAQ-117 (30 min)) after the sample was dissolved in 30 μl of 0.5 M triethylammonium bicarbonate ($N(Et)_3HCO_3$), pH 8.5, and the iTRAQ reagent was dissolved in 70 μl of ethanol. The mixture was incubated at room temperature for 1 h and concentrated to $\sim$20 μl. Samples labeled with four different isotopic iTRAQ reagents were combined and concentrated to 10 μl and then dissolved in 200 μl of IP buffer (100 mM Tris, 100 mM NaCl, and 1% Nonidet P-40, pH 7.4) and 200 μl of water, and pH was adjusted to 7.4. The mixed sample was incubated with 4 μg of immobilized anti-phosphotyrosine antibody (Santa Cruz Biotechnology) overnight at 4 °C. The antibody beads were spun down for 5 min at 7000 rpm, and the supernatant was separated and saved. The antibody-bound beads were washed twice with 200 μl of IP buffer for 10 min and twice with rinse buffer (100 mM Tris, 100 mM NaCl, pH 7.4) for 5 min at room temperature. The phosphotyrosine-containing peptides were eluted from antibody with 50 μl of 100 mM glycine pH 2.5 for 1 h at room temperature.

IMAC and Mass Spectrometry—Phosphopeptide enrichment on IMAC was performed as described previously (14), except that peptides were not converted to methyl esters. After antibody elution, peptides were loaded onto a 10-cm self-packed IMAC (20MC; Applied Biosystems) capillary column (inner diameter, 200 μm; outer diameter, 360 μm) and rinsed with organic rinse solution (25% MeCN, 1% HOAc, 100 mM NaCl) for 10 min at 10 μl/min. The column was equilibrated with 0.1% HOAc for 10 min at 10 μl/min and eluted onto a 10-cm self-packed C18 capillary precolumn (inner diameter, 100 μm; outer diameter, 360 μm) with 50 μl of 250 mM Na_2HPO_4, pH 8.0. After a 10-min rinse (0.1% HOAc), the precolumn was connected to a 10-cm self-packed C18 (YMC-Waters 5 μm ODS-AQ) analytical capillary column (inner diameter, 50 μm; outer diameter, 360 μm) with an integrated electrospray tip ($\sim$1-μm orifice). Peptides were eluted using a 100-min gradient with solvent A (H_2O/HOAc, 99:1 (v/v)) and B (H_2O/MeCN/HOAc, 29:70:1 (v/v)): 10 min from 0% to 15% B, 75 min from 15% to 40% B, and 15 min from 40% to 70% B. Eluted peptides were directly electrosprayed into a Q-TOF mass spectrometer (QSTAR XL Pro; Applied Biosystems). MS/MS spectra of the five most intense peaks with two to five charges in the MS scan were automatically acquired in information-dependent acquisition with previously selected peaks excluded for 40 s.

Western Blot Analysis—40 μg of protein from each sample was mixed with 4× sample buffer (250 mM Tris-HCl, pH 6.8, 8% SDS, 40% glycerol, 0.04% bromphenol blue, and 400 mM dithiothreitol) and boiled for 5 min. Proteins were separated by SDS-PAGE and transferred onto PVDF membranes. After blocking for 1 h at room temper-

Downloaded from www.mcponline.org at Francis A. Countway Library of Medicine on October 16, 2007

ature membranes were incubated overnight at 4 °C in primary antibody, washed three times for 5 min in TBS-Tween 20 (20 mM Tris-HCl, pH 7.5, 137 mM NaCl, and 0.1% Tween 20), incubated for 1 h at room temperature in secondary antibody (dilution 1:2500 horseradish peroxidase conjugated donkey anti-rabbit in TBS-Tween 20, 5% non-fat milk powder) (Amersham Biosciences), and finally washed three times for 5 min with TBS-Tween 20. Blots were developed with ECL Advance Western blotting detection kit (Amersham Biosciences) and scanned on a Kodak Image Station 1000. Primary antibodies used were anti-EGFR, for loading control; anti-EGFR pY1172; anti-Fak pY576; anti-STAT-3 pY705 (all from Cell Signaling Technologies), and anti-Gsk-3-β pY216 (Upstate Biotechnology).

Phosphopeptide Sequencing, Data Clustering, and Analysis—MS/MS spectra were extracted and searched against human protein database (NCBI) using ProQuant (Applied Biosystems) and MASCOT (Matrix Science). For ProQuant, an interrogator database was generated by predigesting the human protein database with trypsin and allowing one miscleavage and up to six modifications on a single peptide (phosphotyrosine $\leq$ 2, phosphoserine $\leq$ 1, phosphothreonine $\leq$ 1, iTRAQ-lysine $\leq$ 4, and iTRAQ-tyrosine $\leq$ 4). Mass tolerance was set to 0.15 atomic mass units for precursor ions and 0.1 atomic mass units for fragment ions. For MASCOT, data were searched against the human non-redundant protein database with trypsin specificity, two missed cleavages, precursor mass tolerance set to 1.5 Da, and fragment ion tolerance set to 0.2 Da. Phosphotyrosine-containing peptides were manually validated and quantified. Peak areas for each of the four signature peaks (*m/z*: 114, 115, 116, 117) were obtained and corrected according to the manufacturer's instructions to account for isotopic overlap. Data were further corrected with values generated from the peak areas of non-phosphorylated peptides to account for possible variations in the starting amounts of sample for each time point. Finally, all data were normalized by the 5-min sample. Mean phosphorylation, standard deviation, and *p* values to estimate statistical significance for differential phosphorylation between the different time points were calculated using Microsoft Excel. The *p* values were calculated using a paired, two-tailed Student's test. A self-organizing map was generated with the Spotfire program to cluster phosphorylation sites with self-similar profiles. All the analyses using Spotfire were done with original built-in functions of the program.

RESULTS

Time-resolved Tyrosine Phosphorylation after EGF Stimulation Measured by Quantitative Mass Spectrometry—Stable-isotope labeling either during cell culture or after cell lysis provides a simple and accurate method for quantifying proteins and peptides from different cell states (22). Stable-isotope-tagged amine-reactive reagents (iTRAQ) from Applied Biosystems enable the comparison of up to four cell states in a single analysis (23). We have combined iTRAQ-based stable isotope labeling of different cell states with immunoprecipitation of tyrosine-phosphorylated peptides (24) to generate a new method enabling quantitative analysis of specific tyrosine phosphorylation sites in four populations of cells subjected to EGF stimulation over different periods of time (0, 5, 10, and 30 min). For each time point, a single 15-cm plate of cells was cultured under the same conditions before stimulation, and EGF (25 nM) was added for the appropriate length of time. Cells were lysed and proteins from each sample were digested with trypsin and desalted. Aliquots corresponding to 20% ($\sim 6 \times 10^6$ cell equivalents) of each of the resulting four sets of peptides were labeled with iTRAQ reagent, mixed together, and immunoprecipitated with anti-phosphotyrosine antibody. Immunoprecipitated, phosphorylated peptides were further enriched by IMAC before LC-MS/MS analysis (Fig. 1*a*). The four iTRAQ labels are nominally isobaric and differ only in the positioning of isotopically tagged atoms. As a result, peptides tagged with the different forms of the reagent co-elute during the LC gradient and generate a single peak for each charge state in the MS scan (23). After selection of a peak in MS mode, MS/MS fragmentation of the iTRAQ labeled peptide results in 4 signatures peaks at *m/z* 114, 115, 116, and 117 respectively (Fig. 1, *b* and *c*), whereas fragmentation along the peptide backbone results in b- and y-type fragment ions, which may be used to identify the peptide sequence (Fig. 1*b*). To facilitate comparison of the temporal phosphorylation profiles, each of the phosphorylation profiles was normalized relative to the 5-min time point because this point typically provided the greatest signal-to-noise ratio; therefore, normalization to this time point minimized noise-associated error. To normalize the results within each sample for protein level and labeling efficiency, the supernatant from the anti-phosphotyrosine peptide immunoprecipitation was analyzed, and iTRAQ marker ions from non-phosphorylated peptides were averaged and used to correct the data (Fig. 1*c*; data available in Supplemental Table III).

Application of this method to investigate EGFR signaling in human mammary epithelial cells resulted in the identification of 78 tyrosine phosphorylation sites on 58 proteins in a single analysis. For each phosphorylation site, a quantitative temporal phosphorylation profile was generated by comparing the relative ratios of peak areas for the iTRAQ marker ions (*m/z* 114–117) in the MS/MS spectrum. The mean values and standard deviations for a subset of the tyrosine phosphorylation sites are provided in Table I along with an estimation of the statistical significance of each value relative to the 5-min time point (a full list of phosphorylation sites, time course phosphorylation profiles, and statistical analysis can be found in Supplemental Table I). For instance, the EGFR pY1172 autophosphorylation site increased 20-fold from 0 to 5 min, decreased by 10% from 5 to 10 min, and decreased by another 40% to 30 min. Based on the number of replicate measurements (as is typical for data-dependent acquisition many of the peptides were selected for MS/MS more than once during the chromatographic elution profile, resulting in multiple independent measurements of the relative ratios for the iTRAQ marker ion peak areas) in the LC/MS/MS analysis, the difference between the 0- and 5-min time points and the 30- and 5-min time points is statistically significant ($p < 0.05$), whereas the difference between the 10- and 5-min time points does not meet this significance criterion for this particular phosphorylation site.

Of the 58 proteins identified in this analysis, 52 have been associated with the EGFR signaling network, whereas the

Downloaded from www.mcponline.org at Francis A. Countway Library of Medicine on October 16, 2007

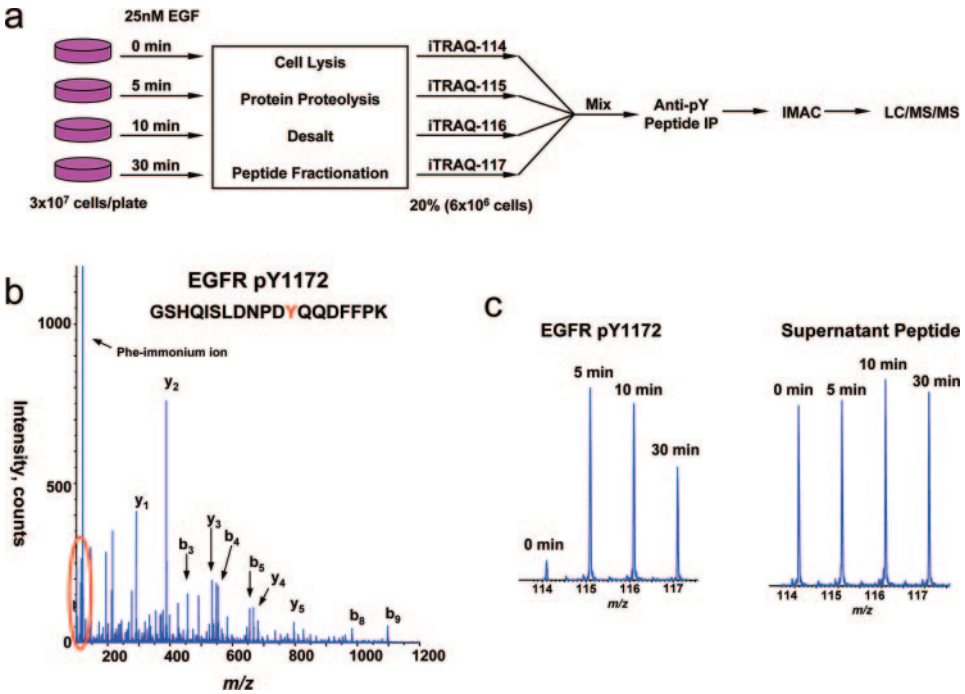

FIG. 1. **Mass spectrometry-based approach to quantitative analysis of phosphorylation dynamics on specific tyrosine residues.** *a*, four plates of cells were cultured under normal conditions, serum-starved for 12 h, and stimulated with 25 nM EGF for 0, 5, 10, or 30 min. After cell lysis, proteins were proteolyzed and the resulting peptide mixture desalted before dividing into aliquots of 10 equivalent fractions per stimulation time. For each stimulation time, one aliquot was labeled with one of the four isoforms of the iTRAQ reagent and then mixed with the labeled aliquots from the other time points. Phosphotyrosine-containing peptides were immunoprecipitated and further enriched by IMAC affinity chromatography before LC/MS/MS analysis. *b*, for each MS/MS spectrum, y- and b-type fragment ions (containing the C and N termini of the peptide, respectively) enable the identification of the peptide sequence including the specific localization of the phosphorylated residue. *c*, quantitative information is encoded in the low mass-to-charge ratio portion of the MS/MS spectrum (highlighted in *b*, *red oval*). The 0-min time point was labeled with iTRAQ-114, the 5-min time point was labeled with iTRAQ-115, the 10-min time point was labeled with iTRAQ-116, and the 30-min time point was labeled with iTRAQ-117. Relative peak areas of the four marker ions were used to quantify tyrosine phosphorylation levels. Protein levels and labeling efficiency were normalized with quantification data generated by analysis of peptides contained in the supernatant after peptide IP. The marker ion region of a representative non-phosphorylated peptide is on the *right side* of *c*.

other six proteins (listed in Table II) have not been previously identified in either proteomic or biochemical analyses of EGFR signaling. Representative spectra for two of the six peptides listed in Table II are presented in Fig. 2; the mass range spanning the iTRAQ marker ion region is highlighted for each peptide. Included in this group of six proteins is KIAA0606, a protein also known as suprachiasmatic nucleus circadian oscillatory protein (SCOP). Regulation of the circadian clock in the suprachiasmatic nucleus drives daily rhythms of behavior and has been associated with EGF receptor signaling in the hypothalamus (25). In addition, EGF activated expression of clock genes *Per1* and *Per2*, and modulation of the circadian rhythm in cell culture has also been documented (26). The mechanism by which signal is transduced from the EGF receptor to the clock gene promoter region has not been elucidated. In this study, we detected rapid and transient tyrosine phosphorylation at pY2060 in SCOP in response to EGF stimulation. This protein and phosphorylation site may be directly involved in signal transduction from activated EGF receptor to downstream up-regulation of clock gene expression, but this relationship needs to be biologically validated. Also included in this group of six proteins is KIAA1217, a protein whose function has not yet been characterized. The specific peptide and phosphorylation site that we have identified on this protein display surprising homology (12/15 identical residues) to a region of p130Cas interacting protein (p140Cap), a protein known to be tyrosine-phosphorylated in response to stimulation with exogenous growth factors (27).

In addition to the six proteins that had not been previously characterized in the EGFR signaling network, we have also identified several novel phosphorylation sites on proteins known to be in the network (a subset of these sites is presented in Table III). Contained in this group are phosphorylation sites on hypothetical protein FLJ00269, hypothetical protein FLJ21610, target of myb1-like 2 protein, and chromosome 3 open reading frame 6 (previously named Ymer by Blagoev *et al.* (19)). Identification and quantification of temporal phosphorylation profiles at specific tyrosine sites in these proteins further confirms the involvement of these proteins in the EGFR signaling cascade and should facilitate biological manipulation of these proteins to help characterize

Downloaded from www.mcponline.org at Francis A. Countway Library of Medicine on October 16, 2007

TABLE I

Quantitative time course tyrosine phosphorylation profiles

A subset of protein phosphorylation sites identified from HMEC cells treated with EGF for varying duration. Results are presented from analysis of two different cell cultures; for the second cell culture, analytical replicates were also performed. The average value is presented in the table. For each protein, specific phosphorylation site(s) were identified and quantified by comparing relative peak areas of the iTRAQ marker ions. The 5-min sample was used to normalize the phosphorylation profiles. The data are therefore presented as a ratio relative to the 5-min time point. Statistical significance was calculated using a paired, two-tailed Student's test.

ID		Quantification: Sample 1, analysis 1			Sample 2, average of analysis 1 and 2		
Protein	Site	Ratio 0 min:5 min	Ratio 10 min:5 min	Ratio 30 min:5 min	Ratio 0 min:5 min	Ratio 10 min:5 min	Ratio 30 min:5 min
c-Cbl	Tyr-552	0.000 ± 0.001***	0.916 ± 0.015	0.365 ± 0.005**	0.028 ± 0.066***	0.715 ± 0.018***	0.314 ± 0.016***
Caveolin 1	Tyr-14	0.391 ± 0.074	1.034 ± 0.009	0.792 ± 0.037	0.425 ± 0.027***	1.121 ± 0.136	0.804 ± 0.061***
EGFR	Tyr-1172	0.050 ± 0.031*	0.900 ± 0.019	0.505 ± 0.012*	0.039 ± 0.021***	0.945 ± 0.109	0.662 ± 0.035***
EGFR	Tyr-1092	0.059	0.744	0.429	0.034 ± 0.016***	0.689 ± 0.111*	0.461 ± 0.095**
EphB1	Tyr-600	0.656 ± 0.090	1.142 ± 0.045	1.064 ± 0.049	0.733 ± 0.038	1.070 ± 0.009	1.182 ± 0.003**
EphrinB2	Tyr-304	0.837	1.364	1.156	0.792 ± 0.153	0.902 ± 0.234	1.072 ± 0.190
EPS15	Tyr-849	0.080	1.409	0.652	0.043 ± 0.050*	1.412 ± 0.130	0.605 ± 0.046
FAK	Tyr-576	0.637 ± 0.051***	1.424 ± 0.051***	1.629 ± 0.036***	0.569 ± 0.088***	0.801 ± 0.076***	1.678 ± 0.206***
FRK	Tyr-497	0.614	1.241	1.340	0.495 ± 0.050*	1.349 ± 0.053	0.773 ± 0.037
GIT 1	Tyr-545	0.575 ± 0.057	1.183 ± 0.016*	1.093 ± 0.040	0.807 ± 0.063*	1.212 ± 0.276	1.074 ± 0.326
GSK-3-β	Tyr-279	0.846 ± 0.014**	1.112 ± 0.024*	0.931 ± 0.028	0.908 ± 0.115	1.147 ± 0.122	0.980 ± 0.082
HER2	Tyr-1248	0.141	0.732	0.532	0.214	0.808	0.492
p130Cas	Tyr-327	1.126	1.136	1.442	2.116 ± 0.130**	1.418 ± 0.058**	1.497 ± 0.045**
ACK1	Tyr-857	0.133	0.997	0.329	0.099 ± 0.037*	0.561 ± 0.069	0.358 ± 0.109
Paxillin	Tyr-118	0.528 ± 0.131	0.755 ± 0.137	0.792 ± 0.164	0.726 ± 0.045***	0.732 ± 0.105**	0.850 ± 0.095*
Plakophilin 3	Tyr-84	0.194	0.778	0.144	0.038 ± 0.007**	0.429 ± 0.015*	0.286 ± 0.023*
PLC-γ	Tyr-775, Tyr-783	0.043	0.605	0.335	0.008 ± 0.016**	0.287 ± 0.013**	0.231 ± 0.001***
PTP NR 11	Tyr-62	0.945 ± 0.032	1.266 ± 0.023*	1.122 ± 0.016	1.074 ± 0.157	0.971 ± 0.142	1.128 ± 0.202
PTPR A	Tyr-798	0.833 ± 0.005*	0.943 ± 0.010	0.708 ± 0.003**	0.873 ± 0.073*	0.740 ± 0.119*	0.613 ± 0.103**
Rho GEF 5	Tyr-19, Tyr-22	0.019 ± 0.037*	0.844 ± 0.052	0.632 ± 0.047	0.000 ± 0.012**	0.352 ± 0.012**	0.248 ± 0.040*
SHC	Tyr-239, 240	0.147 ± 0.015**	1.160 ± 0.083	0.902 ± 0.059	0.173 ± 0.023*	0.995 ± 0.174	0.734 ± 0.198
SHC	Tyr-318	0.028 ± 0.046*	1.077 ± 0.026	0.646 ± 0.003**	0.296 ± 0.392	0.878 ± 0.217	0.908 ± 0.543
SHIP-2	Tyr-986	0.043 ± 0.054***	0.801 ± 0.080	0.363 ± 0.028**	0.013 ± 0.045***	0.428 ± 0.160**	0.291 ± 0.160**
STAM-1	Tyr-381	0.309	2.659	0.926	0.148 ± 0.288*	4.188 ± 0.724**	1.624 ± 0.397
STAM-2	Tyr-374	0.218	2.753	0.908	0.459 ± 0.474	2.515 ± 0.613*	1.308 ± 0.017***
STAT-3 Isoform 1	Tyr-705	0.209 ± 0.026***	0.803 ± 0.073*	0.244 ± 0.046***	0.242 ± 0.092**	0.565 ± .039**	0.478 ± 0.134*
STAT-3 Isofrom2	Tyr-704	0.195	0.794	0.275	0.196 ± 0.197	0.545 ± 0.178	0.406 ± 0.266

*, $p < 0.05$; **, $p < 0.01$; ***, $p < 0.001$.

their functional role in the EGFR network.

To validate the method, we chose to compare our results with those generated by Western blot with phospho-specific antibodies. Four of the phosphorylation sites identified by mass spectrometry were selected; total cell lysate was loaded on the gel and blotted, and selected anti-phosphotyrosine antibodies were used to develop the Western blots. As demonstrated in Fig. 3, anti-phosphotyrosine Western blots recapitulated the general trend measured by mass spectrometry.

As further validation of this data set, a second set of cells were cultured, stimulated with EGF for the appropriate times, lysed, processed, and analyzed to quantify temporal tyrosine phosphorylation profiles. Two replicate analyses were performed on this set of samples to estimate analytical reproducibility of the method, and the iTRAQ labeling scheme was reversed within these replicates to ensure that the quantification was not biased by a particular isoform of the iTRAQ reagent. A subset of the results from these replicate analyses are presented in Table I, and the full data set is contained in Supplemental Table II. Of the 78 tyrosine phosphorylation sites identified from analysis of the first set of cells, 65 were detected and quantified in the analyses of the second set of stimulated cells. The absence of the remaining 13 phosphorylated peptides from the second data set may be due to variation in the efficiency of the immunoprecipitation, but it is more likely to be due to information-dependent acquisition-based selection of peaks for MS/MS analysis. With this mode of operation, it is not surprising that there is some variation in the identification of peptides between analytical (see Supplemental Table II) or biological replicates because the peaks selected for MS/MS will vary from analysis to analysis based on slight shifts in peak selection timing and chromatography. In fact, although 13 tyrosine phosphorylation sites were missed in the analysis of the second set of cells, an additional 26 tyrosine phosphorylation sites were identified with corresponding quantitative temporal phosphorylation profiles (Supplemental Table II).

In addition to providing validation for the data set from the first set of stimulated cells, analysis of a second set of stimulated cells also provided an estimation of the biological variance between the two sets of cell cultures. Similar stimulation conditions should produce similar results, and as expected the majority of the temporal phosphorylation profiles are quite similar between the two biological samples. It is worth noting, however, that some of the profiles show variance in both the level of stimulation (basal (0 min) relative to 5

Downloaded from www.mcponline.org at Francis A. Countway Library of Medicine on October 16, 2007

TABLE II

Tyrosine-phosphorylated proteins not previously reported in EGFR signaling

Of the 58 proteins identified in the analysis of the first biological sample, six have not been previously associated with the EGFR signaling network. Protein identification, tyrosine phosphorylation site, and time course profile data are provided for these six proteins. *, $p < 0.05$; **, $p < 0.01$; ***, $p < 0.001$.

Protein	Site	Ratio		
		0 min:5 min	10 min:5 min	30 min:5 min
Chromosome 20 ORF 18 (HOIL-1)	pY288	0.026 ± 0.034***	1.950 ± 0.156**	0.441 ± 0.012***
Hypothetical protein FLJ14564	pY413	0.66 ± 0.04	0.956 ± 0.063	0.719 ± 0.023
Hypothetical protein FLJ30532 (MARVELD2)	pY23	0.000	0.753	0.534
Retinoic acid induced 3	pY320	0.725 ± 0.117	1.177 ± 0.027	0.891 ± 0.029
KIAA0606 protein	pY2060	0.140	0.671	0.413
KIAA1217 protein	pY393	0.456	1.102	0.952

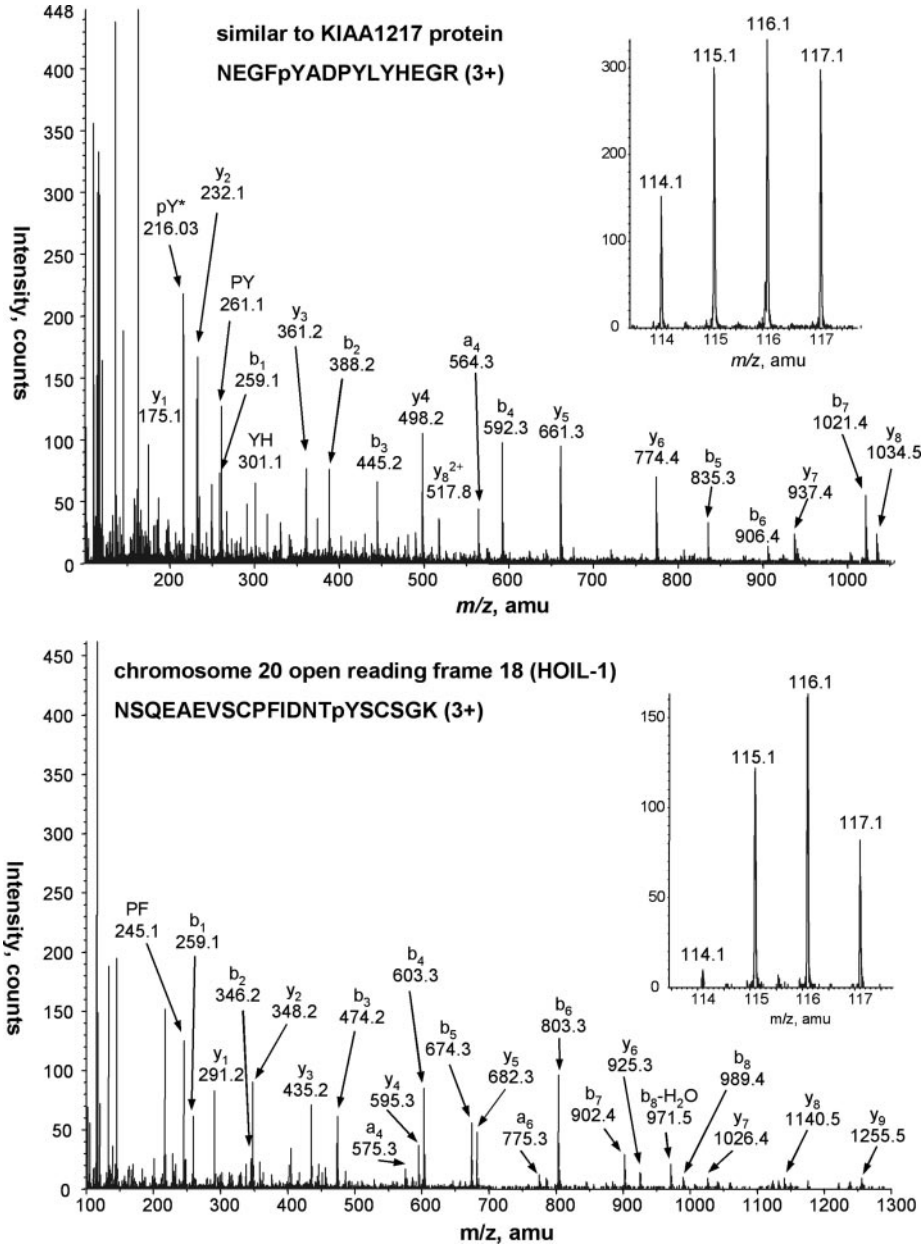

FIG. 2. **Representative MS/MS spectra for two phosphorylated peptides from proteins not previously reported in EGFR signaling.** For each spectrum, y- and b-type fragment ions present in full scan mass spectra enable peptide identification and phosphorylation site assignment, whereas peak areas for each of the iTRAQ marker ions (*inset* for *top* and *bottom*) enable quantification of the temporal phosphorylation profiles.

Downloaded from www.mcponline.org at Francis A. Countway Library of Medicine on October 16, 2007

TABLE III

Tyrosine phosphorylation sites not previously reported in the literature

In addition to the sites listed in Table II, many additional tyrosine phosphorylation sites that have not been previously reported in the literature have been identified in this work. A subset of these sites is presented along with the protein identification and the temporal phosphorylation profile quantification.

Protein	Site	Ratio		
		0 min:5 min	10 min:5 min	30 min:5 min
Hypothetical protein FLJ00269	pY411	0.808	0.841	1.026
Hypothetical protein FLJ21610	pY453	0.261	1.123	0.888
Chromosome 3 ORF 6 (Ymer)	pY145	0.00 ± 0.003***	1.359 ± 0.024*	0.444 ± 0.005**
Target of myb1-like 2	Tyr-160 & Tyr-168	0.059 ± 0.023*	0.640 ± 0.152	0.249 ± 0.058*

*, $p < 0.05$; **, $p < 0.01$; ***, $p < 0.001$.

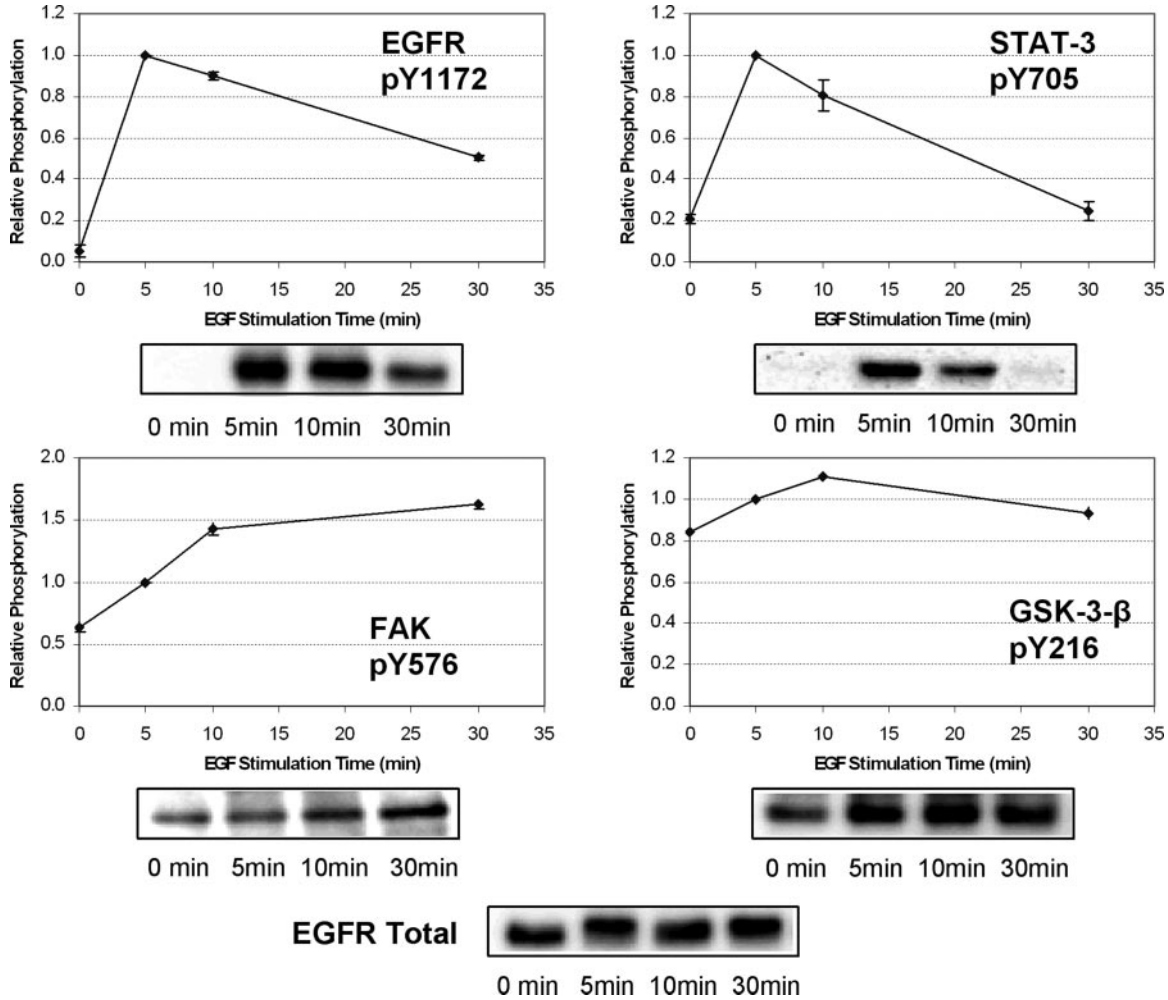

FIG. 3. **Comparison of tyrosine phosphorylation dynamics as measured by mass spectrometry and Western blot analysis.** Tyrosine phosphorylation profiles determined by mass spectrometry were recapitulated by Western blot analysis, further validating the results generated by this approach. Gel loading levels were normalized by probing with an anti-EGFR antibody (*bottom*).

min) and the shape of the temporal profile, perhaps reflecting signaling pathways that are potentiated differently between the two sets of cell cultures. Many possible sources of variation between the cultures exist, including slight changes in the confluence of the cells (different cell-cell contacts would prime signaling pathways differently) and changes in the passage number of the cells (the second set of cells were cultured and stimulated 1 month after the first set of cells). Given the sources of variation, it is not surprising to see slight alteration of the temporal profiles for some of the phosphorylation sites. However, most of the temporal phosphorylation profiles are very similar between the cell cultures, which is indicative of the reproducibility of the method and helps to further validate the results of this study.

Downloaded from www.mcponline.org at Francis A. Countway Library of Medicine on October 16, 2007

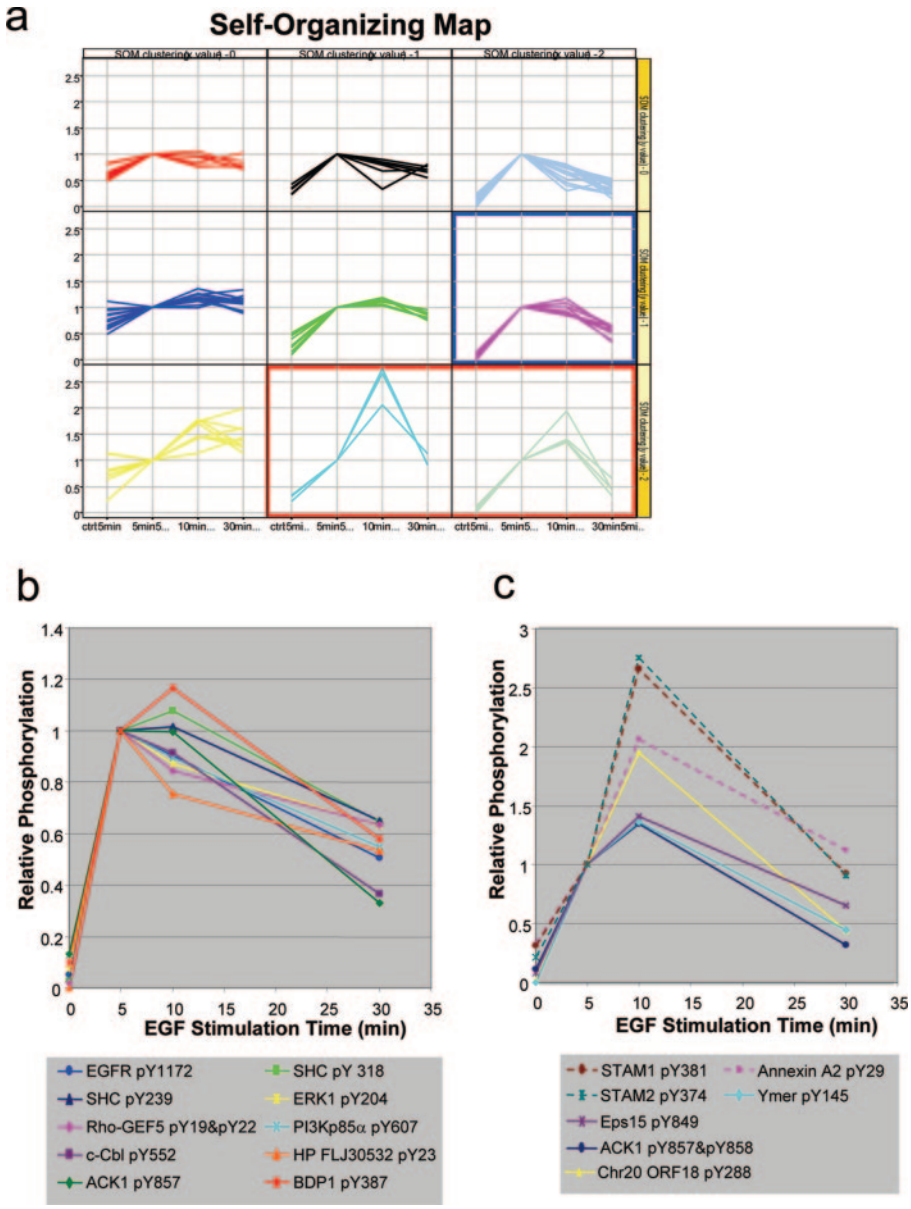

FIG. 4. **SOMs facilitate the identification of EGFR signaling modules.** *a*, after loading the mass spectrometry data into Spotfire, a 3 × 3 self-organizing map was generated to facilitate interpretation of the data and to uncover groups of phosphorylation sites that displayed similar patterns. *b*, a single cluster within the SOM (*blue box*) contained many phosphorylation sites involved in the immediate-early response. *c*, exception for the doubly phosphorylated peptide from ACK1, HOIL-1, and Ymer, phosphorylation sites contained in two adjacent clusters (*red box*) are from proteins implicated in regulation of receptor endocytosis and trafficking. Each of these sites was maximally phosphorylated at 10 min of EGF stimulation. The level of phosphorylation at 10 and 30 min relative to 5 min separated the phosphorylation sites into different compartments.

Bioinformatic Analysis Reveals Dynamic Modules within the EGFR Signaling Network—To ascribe potential functionality to proteins and phosphorylation sites not previously associated with the EGFR signaling network, we attempted to find similar features in temporal phosphorylation profiles between poorly and well characterized protein phosphorylation sites. Sorting through the data manually tends to introduce bias and proved to be time intensive and non-productive. Therefore, with the goal of clustering self-similar phosphorylation profiles (modules) within the EGFR signaling network, we resorted to bioinformatic analysis and generated a self-organizing map (SOM) with the data set from the first set of cells. SOM is a mathematical technique designed to identify underlying patterns in complex data sets; SOMs have been used to analyze gene expression patterns in hematopoietic differentiation, creating biologically relevant clusters and enabling the generation of interesting hypotheses (28). Using the quantitative tyrosine phosphorylation profiles we tested several different options for SOM matrix size before settling on a 3 × 3 matrix (Fig. 4*a*). Smaller matrixes generated clusters that were too complex and difficult to interpret, whereas larger matrixes separated clusters of phosphorylation sites with similar patterns. Clustering self-similar phosphorylation profiles revealed interesting modules in the EGFR signaling network and successfully grouped poorly characterized sites with several well described proteins in the network. For instance, one of the SOM clusters (Fig. 4*b*) has the common profile of a large increase in phosphorylation level from basal to 5 min followed by slow de-phosphorylation from 5 to 10 and 30 min. Included in this cluster is the EGFR pY1172 autophosphorylation site and two

Downloaded from www.mcponline.org at Francis A. Countway Library of Medicine on October 16, 2007

tyrosine phosphorylation sites on SHC, a protein whose PTB (phosphotyrosine-binding) domain binds to EGFR pY1172 (29). In fact, almost all of the phosphorylation sites in this cluster are located on proteins known to interact with EGFR or other receptor tyrosine kinases. For instance, phosphoinositide 3-kinase p85α has been shown to interact (both directly and indirectly) with both EGFR and PDGFR (30). Phosphoinositide 3-kinase p85α pY580 has been ascribed to insulin receptor tyrosine kinase activity (31) but is most probably the result of phosphorylation by EGFR under these stimulation conditions. Other proteins in this group include c-Cbl, Rho-GEF 5, ACK1, BDP1, Erk1, and hypothetical protein FLJ30532, one of the six proteins not previously associated with the EGFR network. c-Cbl is tyrosine-phosphorylated after EGF stimulation and has recently been shown to interact with pY1045 of EGFR after EGF stimulation and before endocytosis of the receptor (32). Tyrosine phosphorylation of activated CDC42 kinase 1 (ACK1) in response to EGF stimulation has been established (33). This protein is most probably localized to the receptor through an interaction with CDC42 and Rho-GEF 5; Rho-GEF proteins have been shown to interact directly with tyrosine kinase receptors (34). BDP1 is a phosphatase involved in regulation of Gab1, mitogen-activated protein kinase, and HER2 signaling after EGF stimulation (35); it is likely that phosphorylation of this protein stimulates phosphatase activity in a negative feedback mechanism.

Erk1 and hypothetical protein FLJ30532, the remaining two proteins in this cluster, are not known to associate directly with EGFR or other receptor tyrosine kinases. From their profiles and grouping in this cluster, the tyrosine phosphorylation sites on these proteins are involved in the immediate early response to EGF stimulation. Hypothetical protein FLJ30532 is also known as MARVELD2, named for MARVEL, a recently discovered tetra-spanning transmembrane domain (36). It is interesting that another MARVEL-domain containing protein has recently been implicated in mediating signal transduction from the B-cell receptor to Erk2 (37). Identification of the tyrosine phosphorylation site on MARVELD2 provides a handle by which to investigate the role of this protein in EGFR-mediated signal transduction, whereas localization to this cluster potentially localizes the topological action of this protein to the immediate-early response to EGF stimulation. It should be noted that although the Erk1 tyrosine site identified in this study is located in the activation loop, the doubly phosphorylated, fully active form of the protein was not detected; this peptide was probably present at a lower level and was below the detection limit of the current approach.

In addition to the immediate-early response module, SOM analysis of the data also uncovered an endocytosis and trafficking module in a metacluster of self-similar time-course phosphorylation profiles found in two adjacent compartments of the SOM (Fig. 4*c*). These phosphorylation sites are all maximally phosphorylated at 10 min after EGF stimulation and have separated into two SOM compartments based on phosphorylation level at 10 min relative to 5 min of stimulation. Proteins within this cluster known to be involved in endocytosis and trafficking included Eps15, STAM1, STAM2, and Annexin A2. EPS15 is necessary for receptor-mediated endocytosis of EGF, and tyrosine phosphorylation of Eps15 after EGF stimulation has been shown (38). Monoubiquitination of Eps15 occurs after EGF-induced internalization of the EGF receptor (39) and may be related to c-Cbl activity, but a phosphorylation site from an alternate E3 ubiquitin-protein ligase, chromosome 20 open reading frame 18 (also known as HOIL-1 (40)) is localized to this cluster and may be responsible for further ubiquitination within the endosomes. Involvement of HOIL-1 in the EGFR pathway has not been characterized, but its biological function fits in well with endocytosis and trafficking. STAM1 and STAM2 phosphorylation sites are also located in these clusters, these proteins bind to ubiquitinated proteins via their Vps27p, Hrs, and STAM domains and ubiquitin-interacting motifs in early endosomes and are involved in endosomal trafficking (41). The N terminus of annexin A2 is tyrosine-phosphorylated after growth factor stimulation and may play a role in receptor trafficking; recently it has been shown that phosphorylation is blocked when receptor internalization is inhibited (42). Based on the clustering of these phosphorylation sites, it is possible that phosphorylation of these sites occurs after EGFR ubiquitination by Cbl and endocytosis via clathrin-coated early endosomes. If so, it may be that Ymer, a protein recently found to be modulated by EGF stimulation (19) and located in these clusters, may be localized to early endosomes. If Ymer follows the role of the other proteins within this cluster, tyrosine phosphorylation of this protein may regulate endosomal trafficking of the receptor. Identification of this regulated site will enable further investigation to determine the functional role of phosphorylation of this protein in EGFR signaling.

DISCUSSION

Quantitative, time-resolved analysis of phosphorylated-tyrosine mediated signaling cascades downstream of activated receptor tyrosine kinases will be critical in developing a better understanding of the molecular mechanisms underlying a variety of disease states. To this end, the method that we have developed has enabled the quantification of the temporal phosphorylation profile of specific tyrosine phosphorylation sites after EGF stimulation. This method is not limited to EGFR signaling but is applicable to the investigation of a broad variety of other tyrosine-mediated signal transduction pathways. Stable-isotope labeling of peptides with the iTRAQ reagent occurs after cell lysis and tryptic digestion but before immunoprecipitation. Quantification is therefore not limited to cell culture-derived samples, and variations in immunoprecipitation do not affect quantification. In fact, because only several hundred micrograms of protein is required per sample per analysis, this method should be readily amenable to the

Downloaded from www.mcponline.org at Francis A. Countway Library of Medicine on October 16, 2007

investigation of signal transduction in samples with limited quantities of protein, such as clinical tumor tissues.

It is worth noting that Blagoev *et al.* (19) have recently published an alternative method combining stable isotope labeling with amino acids in cell culture and immunoprecipitation of tyrosine-phosphorylated proteins, thereby enabling the quantification of temporal involvement in the EGFR signaling network at the protein level. Although the two methods seem quite similar, there are important advantages and disadvantages of each that should be noted. The method that we describe here provides identification of specific protein phosphorylation sites and quantitative temporal phosphorylation profiles for each of these sites; the method of Blagoev *et al.* (19) monitors tyrosine phosphorylation (or association with tyrosine-phosphorylated proteins) at the protein level without site specification. Our site-specific monitoring of protein phosphorylation provides more explicit detail regarding the regulation of proteins within the network but precludes analysis of potential other, non-phosphorylated proteins associated (and therefore co-immunoprecipitated) with tyrosine-phosphorylated proteins. In both methods, only those peptides (and therefore proteins) amenable to LC/MS/MS analysis will be identified; this limitation is more significant for peptide-immunoprecipitation in that there are fewer peptides with which to identify each protein. Our current method uses only a single anti-phosphotyrosine antibody such that the results may be constrained by the bias associated with this particular antibody. Future work will investigate the use of multiple different antibodies to increase coverage of the network. Despite differences between the two methods, there is significant consistency at the protein level between the Blagoev *et al.* (19) data set and our data set, with ours then providing additional site-specific information. Differences in the temporal phosphorylation profiles between the two studies are probably caused by multiple tyrosine phosphorylation sites on a given protein but may also be caused by the different quantification methods (stable isotope labeling with amino acids in cell culture *versus* iTRAQ).

Another study using anti-phosphotyrosine protein immunoprecipitation, stable isotope (ICAT) labeling, and mass spectrometry to study EGFR signaling was recently published (43). Similar to Blagoev *et al.* (19), Thelemann *et al.* (43) monitored tyrosine phosphorylation (or association with tyrosine-phosphorylated proteins) at the protein level without site specification, although many phosphorylation sites were identified without stable-isotope quantification in a separate section of the manuscript. It is difficult to directly compare our data with those reported by Thelemann *et al.* (43) because the total number of proteins quantified in their report was significantly fewer than contained in either our data set or the data set reported by Blagoev *et al.* (19).

In this article, we have demonstrated an analytical method enabling the quantification of time-resolved tyrosine phosphorylation profiles with site-specific resolution and estimated the statistical significance of the relative phosphorylation levels at each time point after stimulation. Data generated by this method self-organize into clusters of phosphorylation sites that recapitulate and extend biological findings in the literature. Generation of an SOM has enabled the identification of modules in the EGFR signaling network. Based on the presence of particular proteins within these modules, we can generate additional hypotheses aimed at defining the potential function of tyrosine phosphorylation on several proteins not previously implicated in EGFR signaling. Further analysis and modeling of the data generated in this study are likely to result in the development of more sophisticated models of receptor-initiated signal transduction, endocytosis, trafficking, and regulation. Future application of this method to interrogate aberrant signaling downstream of constitutively active tyrosine kinases may reveal mechanisms of pathogenesis in these systems, and may provide additional targets for novel therapeutics.

Acknowledgments—We thank Rebecca Fry for assistance with the SpotFire program and other members of the White and Lauffenburger laboratories for helpful discussions.

* This work was supported by NCI, National Institutes of Health, Bioengineering Research Partnership Grant CA96504 (to D. A. L) and National Institutes of Health Grants GM68762 (to D. A. L.), DK070172 (to F. M. W.), and DK42816 (to F. M. W.). The costs of publication of this article were defrayed in part by the payment of page charges. This article must therefore be hereby marked "*advertisement*" in accordance with 18 U.S.C. Section 1734 solely to indicate this fact.

[S] The on-line version of this article (available at http://www.mcponline.org) contains Supplemental Tables I–III.

§ Both authors contributed equally to this work.

** To whom correspondence should be addressed: Biological Engineering Division, 56-787, MIT, Cambridge, MA 02139. Tel.: 617-258-8949; E-mail: fwhite@mit.edu.

REFERENCES

1. Holbro, T., and Hynes, N. E. (2004) ErbB receptors: directing key signaling networks throughout life. *Annu. Rev. Pharmacol. Toxicol.* **44,** 195–217
2. Batzer, A. G., Rotin, D., Urena, J. M., Skolnik, E. Y., and Schlessinger, J. (1994) Hierarchy of binding sites for Grb2 and Shc on the epidermal growth factor receptor. *Mol. Cell. Biol.* **14,** 5192–5201
3. Okabayashi, Y., Kido, Y., Okutani, T., Sugimoto, Y., Sakaguchi, K., and Kasuga, M. (1994) Tyrosines 1148 and 1173 of activated human epidermal growth factor receptors are binding sites of Shc in intact cells. *J. Biol. Chem.* **269,** 18674–18678
4. Navolanic, P. M., Steelman, L. S., and McCubrey, J. A. (2003) EGFR family signaling and its association with breast cancer development and resistance to chemotherapy. *Int. J. Oncol.* **22,** 237–252
5. Schoeberl, B., Eichler-Jonsson, C., Gilles, E. D., and Muller, G. (2002) Computational modeling of the dynamics of the MAP kinase cascade activated by surface and internalized EGF receptors. *Nat. Biotechnol.* **20,** 370–375
6. Wells, A., Ware, M. F., Allen, F. D., and Lauffenburger, D. A. (1999) Shaping up for shipping out: PLCgamma signaling of morphology changes in EGF-stimulated fibroblast migration. *Cell Motil. Cytoskel.* **44,** 227–233
7. Moro, L., Dolce, L., Cabodi, S., Bergatto, E., Erba, E. B., Smeriglio, M., Turco, E., Retta, S. F., Giuffrida, M. G., Venturino, M., Godovac-Zimmermann, J., Conti, A., Schaefer, E., Beguinot, L., Tacchetti, C., Gaggini, P., Silengo, L., Tarone, G., and Defilippi, P. (2002) Integrin-induced epidermal growth factor (EGF) receptor activation requires c-Src and p130Cas and leads to phosphorylation of specific EGF receptor tyrosines. *J. Biol.*

Downloaded from www.mcponline.org at Francis A. Countway Library of Medicine on October 16, 2007

Chem. **277,** 9405–9414
8. Gotoh, N., Toyoda, M., and Shibuya, M. (1997) Tyrosine phosphorylation sites at amino acids 239 and 240 of Shc are involved in epidermal growth factor-induced mitogenic signaling that is distinct from Ras/mitogen-activated protein kinase activation. *Mol. Cell. Biol.* **17,** 1824–1831
9. Irish, J. M., Hovland, R., Krutzik, P. O., Perez, O. D., Bruserud, O., Gjertsen, B. T., and Nolan, G. P. (2004) Single cell profiling of potentiated phospho-protein networks in cancer cells. *Cell* **118,** 217–228
10. Krutzik, P. O., Irish, J. M., Nolan, G. P., and Perez, O. D. (2004) Analysis of protein phosphorylation and cellular signaling events by flow cytometry: techniques and clinical applications. *Clin. Immunol.* **110,** 206–221
11. Beausoleil, S. A., Jedrychowski, M., Schwartz, D., Elias, J. E., Villen, J., Li, J., Cohn, M. A., Cantley, L. C., and Gygi, S. P. (2004) Large-scale characterization of HeLa cell nuclear phosphoproteins. *Proc. Natl. Acad. Sci. U. S. A.* **101,** 12130–12135
12. Brill, L. M., Salomon, A. R., Ficarro, S. B., Mukherji, M., Stettler-Gill, M., and Peters, E. C. (2004) Robust phosphoproteomic profiling of tyrosine phosphorylation sites from human T cells using immobilized metal affinity chromatography and tandem mass spectrometry. *Anal. Chem.* **76,** 2763–2772
13. Salomon, A. R., Ficarro, S. B., Brill, L. M., Brinker, A., Phung, Q. T., Ericson, C., Sauer, K., Brock, A., Horn, D. M., Schultz, P. G., and Peters, E. C. (2003) Profiling of tyrosine phosphorylation pathways in human cells using mass spectrometry. *Proc. Natl. Acad. Sci. U. S. A.* **100,** 443–448
14. Ficarro, S. B., McCleland, M. L., Stukenberg, P. T., Burke, D. J., Ross, M. M., Shabanowitz, J., Hunt, D. F., and White, F. M. (2002) Phosphoproteome analysis by mass spectrometry and its application to *Saccharomyces cerevisiae. Nat. Biotechnol.* **20,** 301–305
15. Steen, H., Kuster, B., Fernandez, M., Pandey, A., and Mann, M. (2002) Tyrosine phosphorylation mapping of the epidermal growth factor receptor signaling pathway. *J. Biol. Chem.* **277,** 1031–1039
16. Hinsby, A. M., Olsen, J. V., Bennett, K. L., and Mann, M. (2003) Signaling initiated by overexpression of the fibroblast growth factor receptor-1 investigated by mass spectrometry. *Mol. Cell. Proteomics* **2,** 29–36
17. Pandey, A., Blagoev, B., Kratchmarova, I., Fernandez, M., Nielsen, M., Kristiansen, T. Z., Ohara, O., Podtelejnikov, A. V., Roche, S., Lodish, H. F., and Mann, M. (2002) Cloning of a novel phosphotyrosine binding domain containing molecule, Odin, involved in signaling by receptor tyrosine kinases. *Oncogene* **21,** 8029–8036
18. Pandey, A., Podtelejnikov, A. V., Blagoev, B., Bustelo, X. R., Mann, M., and Lodish, H. F. (2000) Analysis of receptor signaling pathways by mass spectrometry: identification of vav-2 as a substrate of the epidermal and platelet-derived growth factor receptors. *Proc. Natl. Acad. Sci. U. S. A.* **97,** 179–184
19. Blagoev, B., Ong, S. E., Kratchmarova, I., and Mann, M. (2004) Temporal analysis of phosphotyrosine-dependent signaling networks by quantitative proteomics. *Nat Biotechnol* **22,** 1139–1145
20. Stampfer, M. R., and Bartley, J. C. (1985) Induction of transformation and continuous cell lines from normal human mammary epithelial cells after exposure to benzo[a]pyrene. *Proc. Natl. Acad. Sci. U. S. A.* **82,** 2394–2398
21. Hendriks, B. S., Opresko, L. K., Wiley, H. S., and Lauffenburger, D. (2003) Coregulation of epidermal growth factor receptor/human epidermal growth factor receptor 2 (HER2) levels and locations: quantitative analysis of HER2 overexpression effects. *Cancer Res.* **63,** 1130–1137
22. Ong, S. E., Blagoev, B., Kratchmarova, I., Kristensen, D. B., Steen, H., Pandey, A., and Mann, M. (2002) Stable isotope labeling by amino acids in cell culture, SILAC, as a simple and accurate approach to expression proteomics. *Mol. Cell. Proteomics* **1,** 376–386
23. Ross, P. L., Huang, Y. N., Marchese, J., Williamson, B., Parker, K., Hattan, S., Khainovski, N., Pillai, S., Dey, S., Daniels, S., Purkayastha, S., Juhasz, P., Martin, S., Bartlet-Jones, M., He, F., Jacobson, A., and Pappin, D. (2004) Multiplexed protein quantitation in *saccharomyces cerevisiae* using amine-reactive isobaric tagging reagents. *Mol. Cell. Proteomics*
24. Rush, J., Moritz, A., Lee, K. A., Guo, A., Goss, V. L., Spek, E. J., Zhang, H., Zha, X. M., Polakiewicz, R. D., and Comb, M. J. (2004) Immunoaffinity profiling of tyrosine phosphorylation in cancer cells. *Nat. Biotechnol.* **23,** 94–101
25. Kramer, A., Yang, F. C., Snodgrass, P., Li, X., Scammell, T. E., Davis, F. C., and Weitz, C. J. (2003) Regulation of daily locomotor activity and sleep by hypothalamic EGF receptor signalling. *Novartis Found. Symp.* **253,** 250–262; discussion 102–259, 263–256, 281–254
26. Balsalobre, A., Marcacci, L., and Schibler, U. (2000) Multiple signaling pathways elicit circadian gene expression in cultured Rat-1 fibroblasts. *Curr. Biol.* **10,** 1291–1294
27. Di Stefano, P., Cabodi, S., Boeri Erba, E., Margaria, V., Bergatto, E., Giuffrida, M. G., Silengo, L., Tarone, G., Turco, E., and Defilippi, P. (2004) P130Cas-associated protein (p140Cap) as a new tyrosine-phosphorylated protein involved in cell spreading. *Mol. Biol. Cell* **15,** 787–800
28. Tamayo, P., Slonim, D., Mesirov, J., Zhu, Q., Kitareewan, S., Dmitrovsky, E., Lander, E. S., and Golub, T. R. (1999) Interpreting patterns of gene expression with self-organizing maps: methods and application to hematopoietic differentiation. *Proc. Natl. Acad. Sci. U. S. A.* **96,** 2907–2912
29. Sakaguchi, K., Okabayashi, Y., Kido, Y., Kimura, S., Matsumura, Y., Inushima, K., and Kasuga, M. (1998) Shc phosphotyrosine-binding domain dominantly interacts with epidermal growth factor receptors and mediates Ras activation in intact cells. *Mol. Endocrinol.* **12,** 536–543
30. Hu, P., Margolis, B., Skolnik, E. Y., Lammers, R., Ullrich, A., and Schlessinger, J. (1992) Interaction of phosphatidylinositol 3-kinase-associated p85 with epidermal growth factor and platelet-derived growth factor receptors. *Mol. Cell. Biol.* **12,** 981–990
31. Hayashi, H., Nishioka, Y., Kamohara, S., Kanai, F., Ishii, K., Fukui, Y., Shibasaki, F., Takenawa, T., Kido, H., and Katsunuma, N. (1993) The alpha-type 85-kDa subunit of phosphatidylinositol 3-kinase is phosphorylated at tyrosines 368, 580, and 607 by the insulin receptor. *J. Biol. Chem.* **268,** 7107–7117
32. Grovdal, L. M., Stang, E., Sorkin, A., and Madshus, I. H. (2004) Direct interaction of Cbl with pTyr 1045 of the EGF receptor (EGFR) is required to sort the EGFR to lysosomes for degradation. *Exp. Cell Res.* **300,** 388–395
33. Satoh, T., Kato, J., Nishida, K., and Kaziro, Y. (1996) Tyrosine phosphorylation of ACK in response to temperature shift-down, hyperosmotic shock, and epidermal growth factor stimulation. *FEBS Lett.* **386,** 230–234
34. Taya, S., Inagaki, N., Sengiku, H., Makino, H., Iwamatsu, A., Urakawa, I., Nagao, K., Kataoka, S., and Kaibuchi, K. (2001) Direct interaction of insulin-like growth factor-1 receptor with leukemia-associated RhoGEF. *J. Cell Biol.* **155,** 809–820
35. Gensler, M., Buschbeck, M., and Ullrich, A. (2004) Negative regulation of HER2 signaling by the PEST-type protein-tyrosine phosphatase BDP1. *J. Biol. Chem.* **279,** 12110–12116
36. Sanchez-Pulido, L., Martin-Belmonte, F., Valencia, A., and Alonso, M. A. (2002) MARVEL: a conserved domain involved in membrane apposition events. *Trends Biochem. Sci.* **27,** 599–601
37. Imamura, Y., Katahira, T., and Kitamura, D. (2004) Identification and characterization of a novel BASH N terminus-associated protein, BNAS2. *J. Biol. Chem.* **279,** 26425–26432
38. Salcini, A. E., Chen, H., Iannolo, G., De Camilli, P., and Di Fiore, P. P. (1999) Epidermal growth factor pathway substrate 15, Eps15. *Int. J. Biochem. Cell Biol.* **31,** 805–809
39. van Delft, S., Govers, R., Strous, G. J., Verkleij, A. J., and van Bergen en Henegouwen, P. M. (1997) Epidermal growth factor induces ubiquitination of Eps15. *J. Biol. Chem.* **272,** 14013–14016
40. Yamanaka, K., Ishikawa, H., Megumi, Y., Tokunaga, F., Kanie, M., Rouault, T. A., Morishima, I., Minato, N., Ishimori, K., and Iwai, K. (2003) Identification of the ubiquitin-protein ligase that recognizes oxidized IRP2. *Nat. Cell Biol.* **5,** 336–340
41. Mizuno, E., Kawahata, K., Kato, M., Kitamura, N., and Komada, M. (2003) STAM proteins bind ubiquitinated proteins on the early endosome via the VHS domain and ubiquitin-interacting motif. *Mol. Biol. Cell* **14,** 3675–3689
42. Biener, Y., Feinstein, R., Mayak, M., Kaburagi, Y., Kadowaki, T., and Zick, Y. (1996) Annexin II is a novel player in insulin signal transduction. Possible association between annexin II phosphorylation and insulin receptor internalization. *J. Biol. Chem.* **271,** 29489–29496
43. Thelemann, A., Petti, F., Griffin, G., Iwata, K., Hunt, T., Settinari, T., Fenyo, D., Gibson, N., and Haley, J. D. (2005) Phosphotyrosine signaling networks in epidermal growth factor receptor overexpressing squamous carcinoma cells. *Mol. Cell. Proteomics* **4,** 356–376

Downloaded from www.mcponline.org at Francis A. Countway Library of Medicine on October 16, 2007